

# **Supporting Information for**

# **Exploration of NaSICON Frameworks as**

# **Calcium-ion Battery Electrodes**

Dereje Bekele Tekliye<sup>a</sup>, Ankit Kumar<sup>a</sup>, Xie Weihang<sup>b</sup>, Thelakkattu Devassy Mercy<sup>c</sup>,

Pieremanuele Canepa<sup>b,d</sup>, Gopalakrishnan Sai Gautam<sup>a,\*</sup>

<sup>a</sup>Department of Materials Engineering, Indian Institute of Science, Bengaluru, 560012,  
Karnataka, India

<sup>b</sup>Department of Materials Science and Engineering, National University of Singapore,  
Singapore 117575, Singapore

<sup>c</sup>Vikram Sarabhai Space Centre, Thiruvananthapuram, 695022, Kerala, India

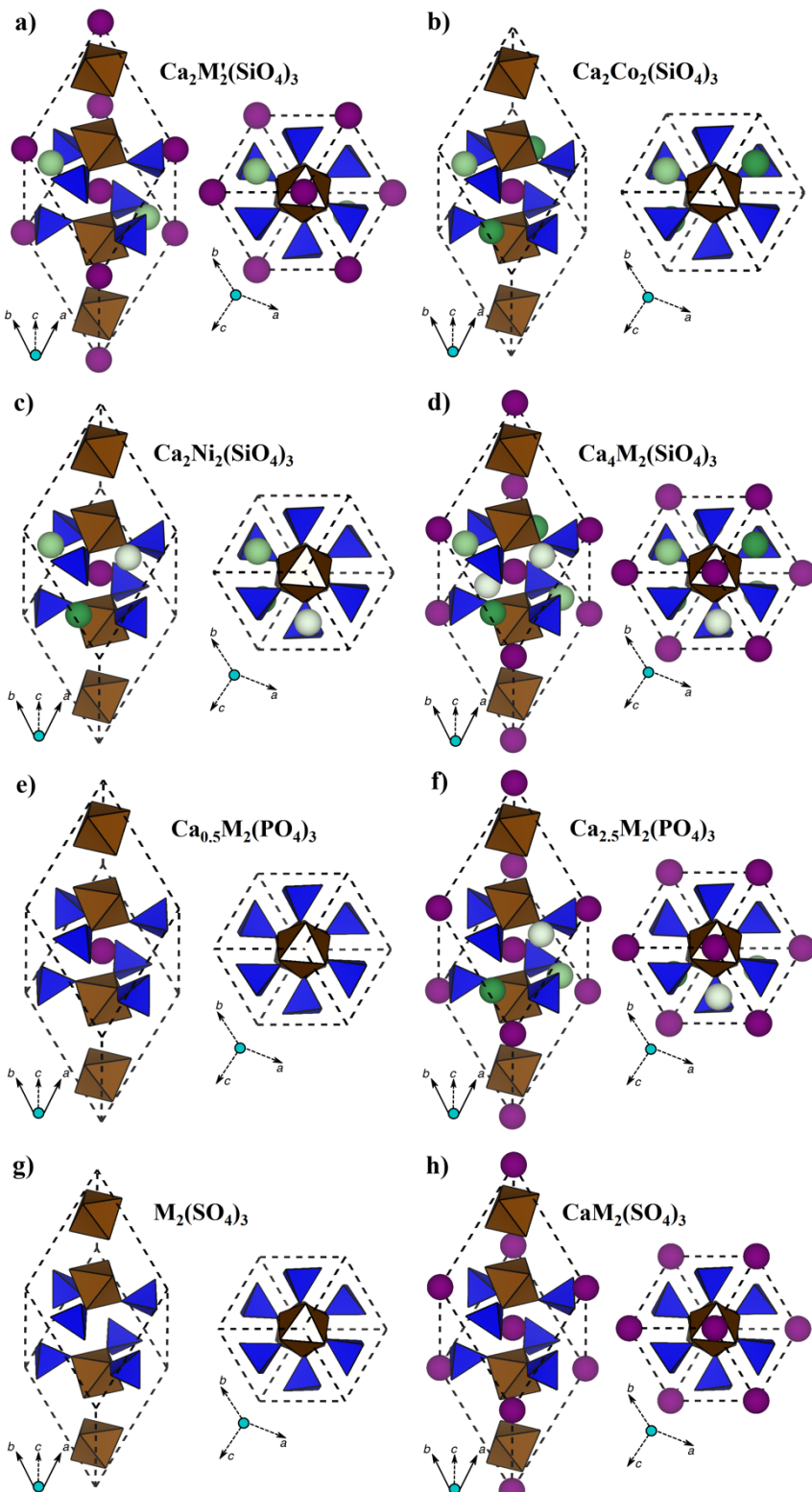
<sup>d</sup>Department of Chemical and Biomolecular Engineering, National University of Singapore,  
Singapore 117575, Singapore

\*E-mail: [saigautamg@iisc.ac.in](mailto:saigautamg@iisc.ac.in)

## **POTCARs used**

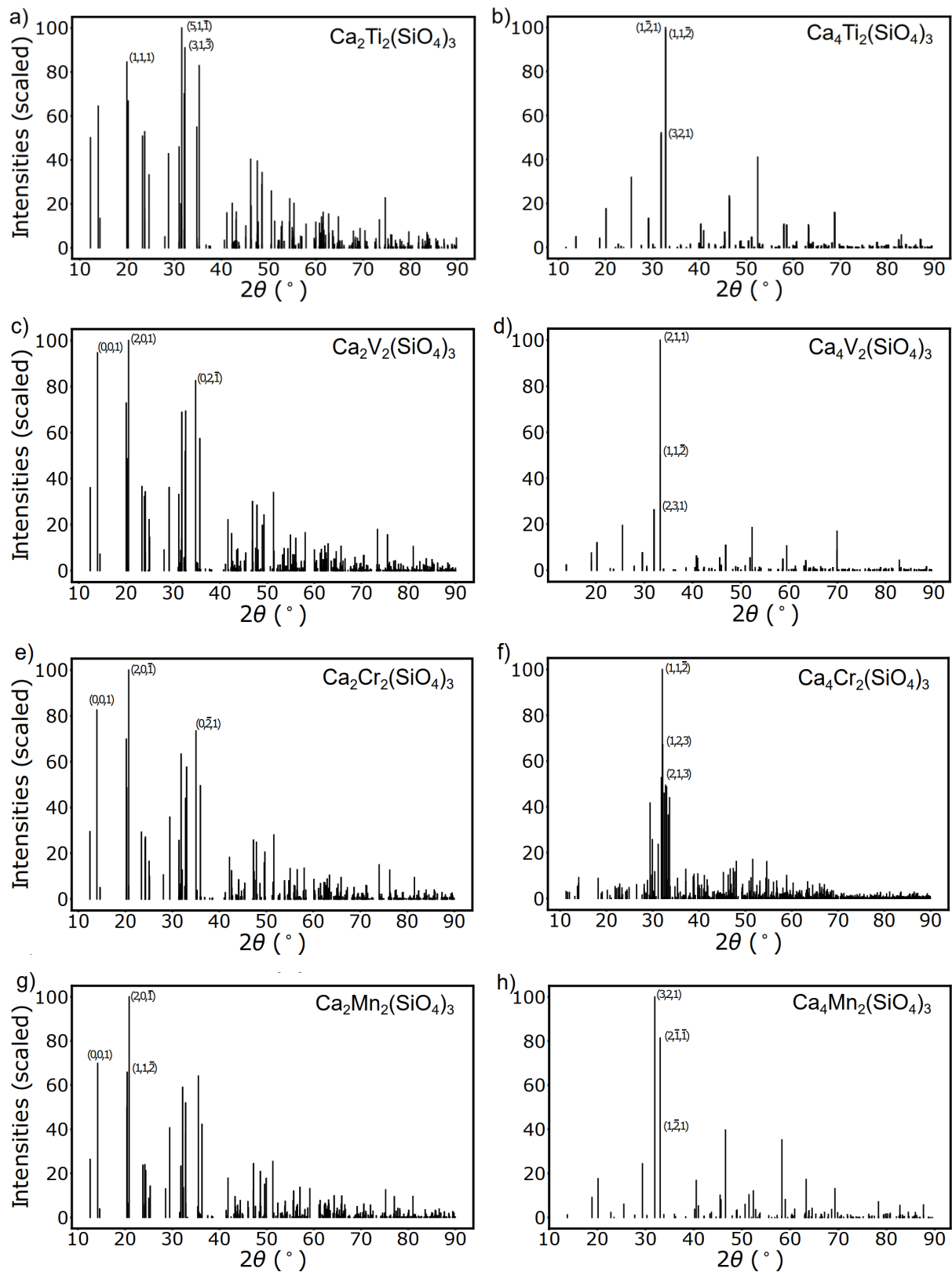
To describe the core electrons of each atomic species the following projector augmented wave (PAW) potentials were used: Ca\_sv 06Sep2000, Ti\_pv 07Sep2000, V\_pv 07Sep2000, Cr\_pv 02Aug2007, Mn\_pv 02Aug2007, Fe\_pv 02Aug2007, Co\_pv 23Apr2009, Ni\_pv 06Sep2000, Si 05Jan2001, P 06Sep2000, S 06Sep2000, and O 08Apr2002.

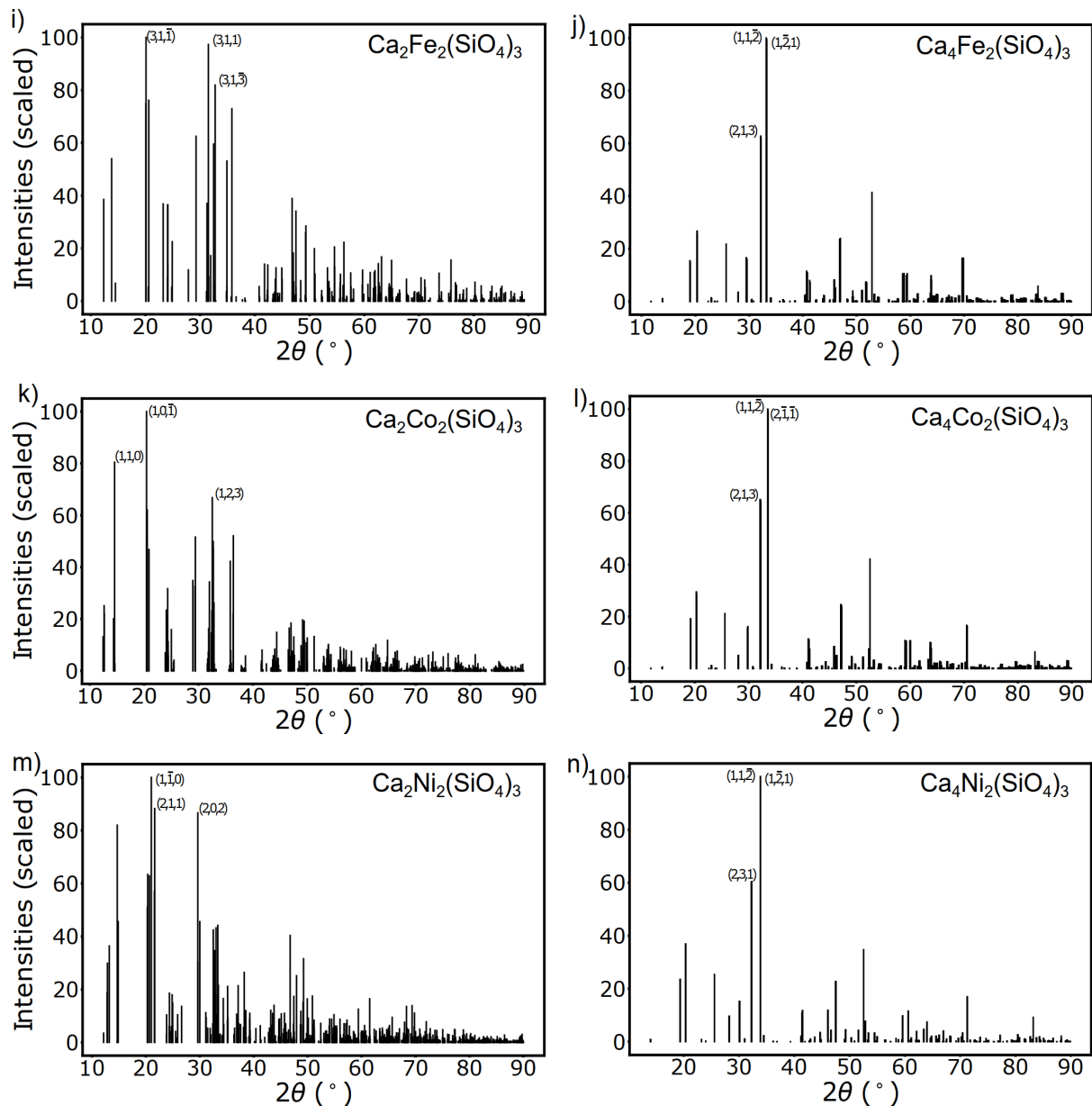
## Structural features of $\text{Ca}_x\text{M}_2(\text{SiO}_4)_3$ , $\text{Ca}_x\text{M}_2(\text{PO}_4)_3$ , and $\text{Ca}_x\text{M}_2(\text{SO}_4)_3$



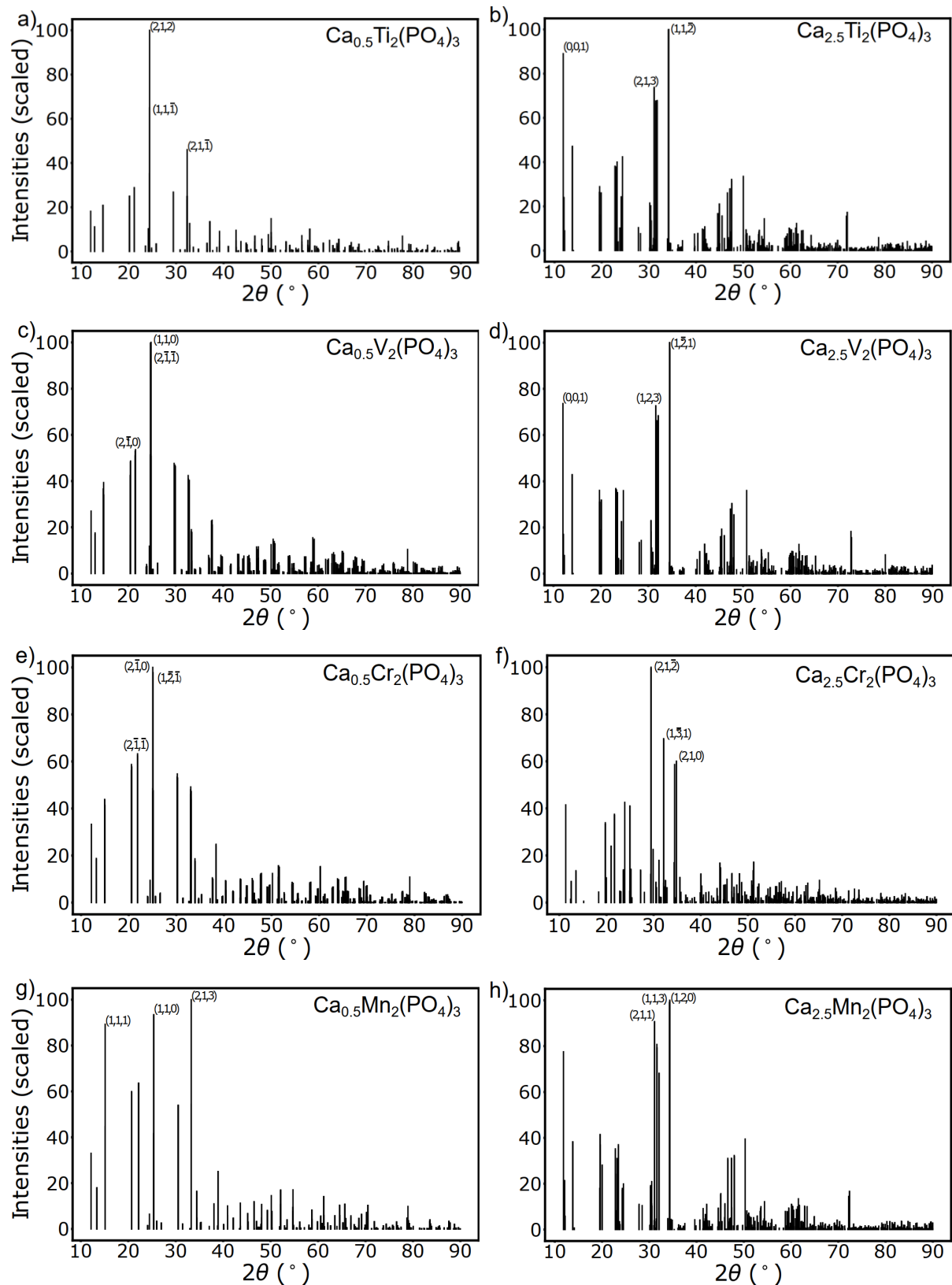
**Figure S1** The crystal structure of (a)  $\text{Ca}_2\text{M}'_2(\text{SiO}_4)_3$ , (b)  $\text{Ca}_2\text{Co}_2(\text{SiO}_4)_3$ , (c)  $\text{Ca}_2\text{Ni}_2(\text{SiO}_4)_3$ , (d)  $\text{Ca}_4\text{M}_2(\text{SiO}_4)_3$ , (e)  $\text{Ca}_{0.5}\text{M}_2(\text{PO}_4)_3$ , (f)  $\text{Ca}_{2.5}\text{M}_2(\text{PO}_4)_3$ , (g)  $\text{M}_2(\text{SO}_4)_3$ , and (h)  $\text{CaM}_2(\text{SO}_4)_3$ , where  $\text{M} = \text{Ti}, \text{V}, \text{Cr}, \text{Mn}, \text{Fe}, \text{Co}$  or  $\text{Ni}$ , and  $\text{M}' = \text{Ti}, \text{V}, \text{Cr}, \text{Mn}$ , or  $\text{Fe}$ . The  $\text{MO}_6$ , and  $\text{ZO}_4$  ( $\text{Z} = \text{Si}, \text{P}$ , or  $\text{S}$ ), polyhedra are indicated by brown and blue colours, respectively. Purple spheres are  $\text{Ca}1$  sites. Green-shaded spheres are  $\text{Ca}2$  sites.

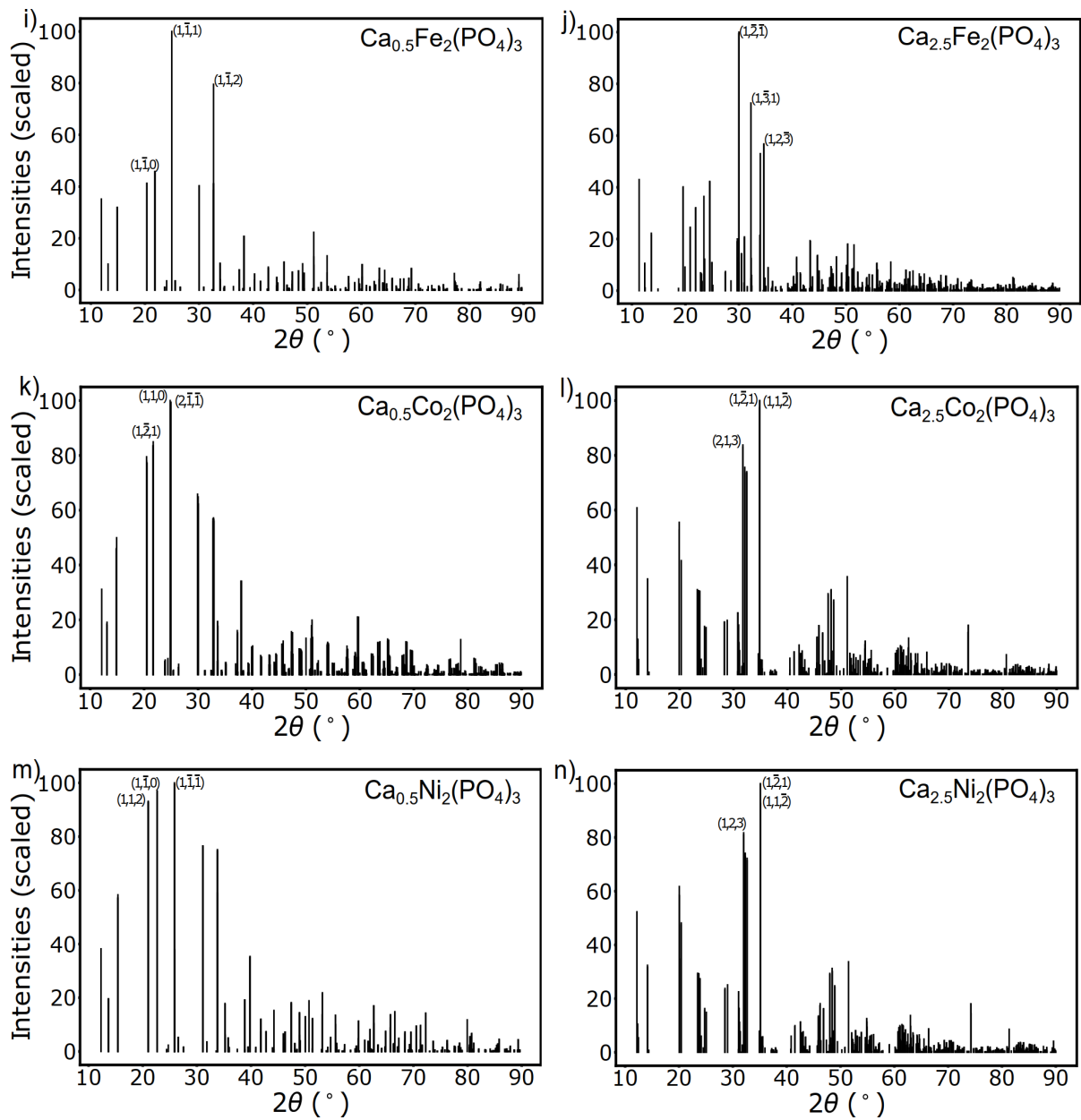
## Simulated X-ray diffraction (XRD) patterns for all Ca-NaSICON compositions



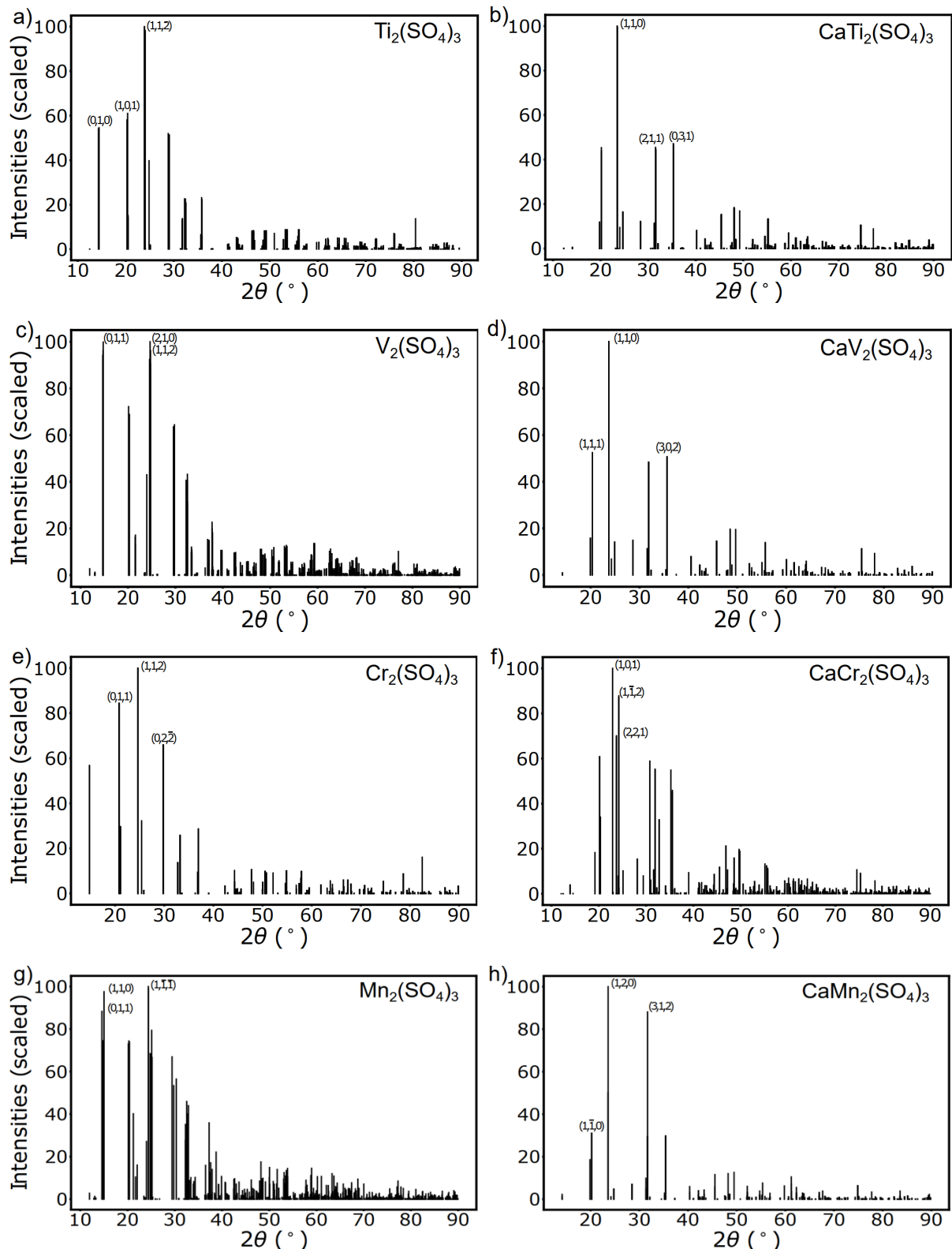


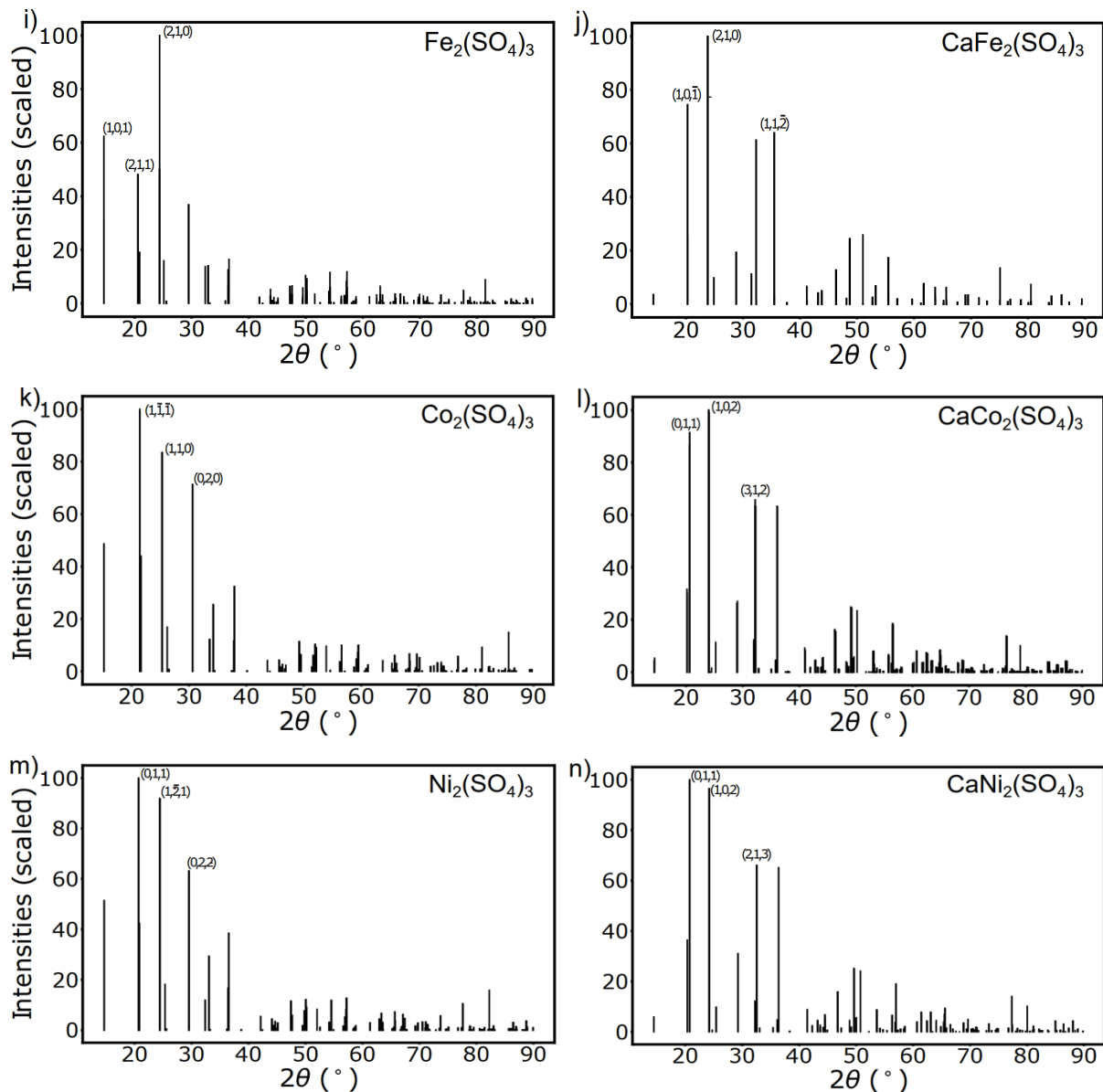
**Figure S2:** Simulated XRD patterns of charged (panels a, c, e, g, i, k, m) and discharged (b, d, f, h, j, l, n) Ti, V, Cr, Mn, Fe, Co, and Ni silicate Ca-NaSICONs. The top three highest intensity low angle peaks are indexed by their Miller indices. Cu K $\alpha$  wavelength is used for all calculations.





**Figure S3:** Simulated XRD patterns of charged (panels a, c, e, g, i, k, m) and discharged (b, d, f, h, j, l, n) Ti, V, Cr, Mn, Fe, Co, and Ni phosphate Ca-NaSICONs. Notations in the figure are identical to **Figure S2**.

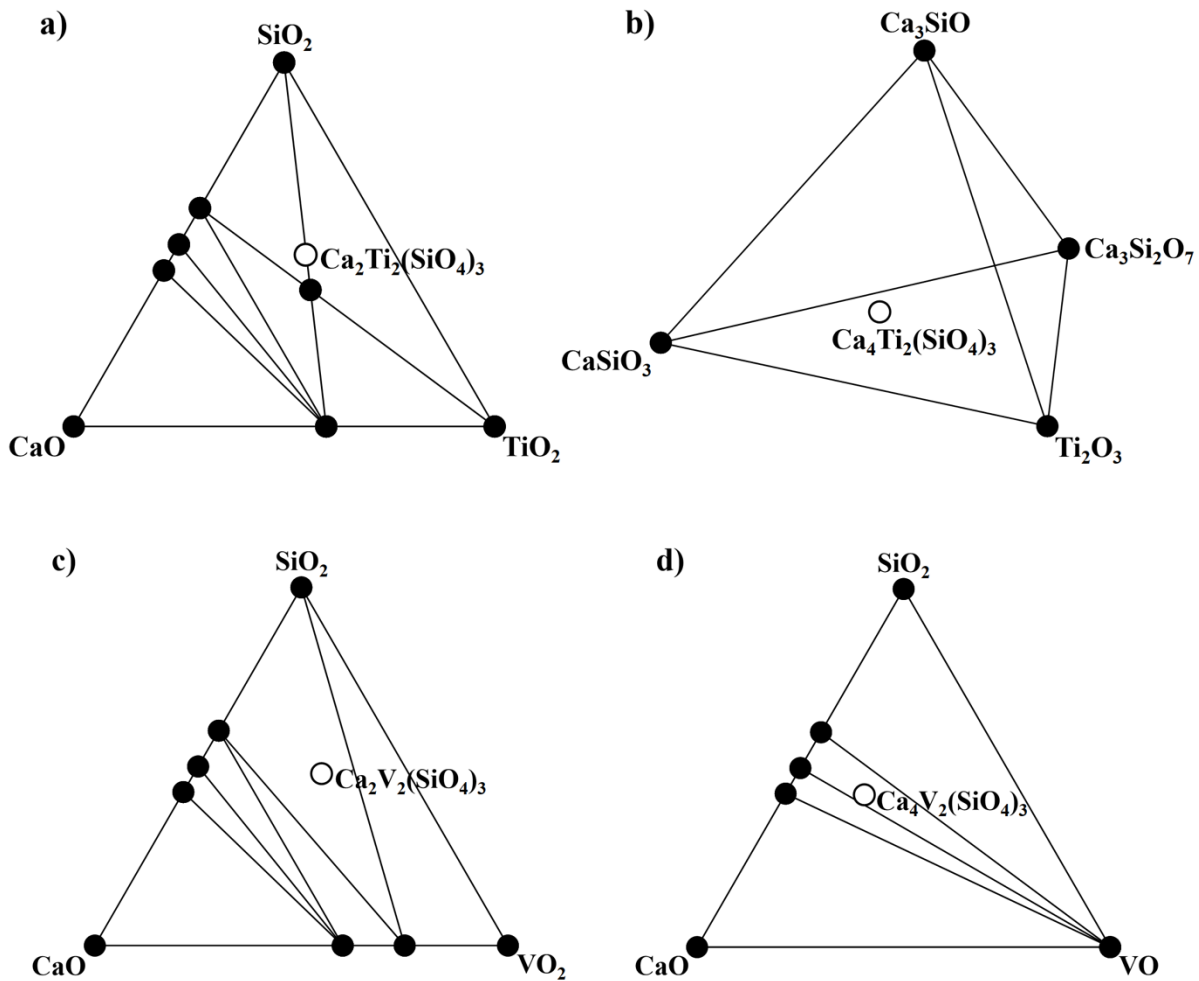


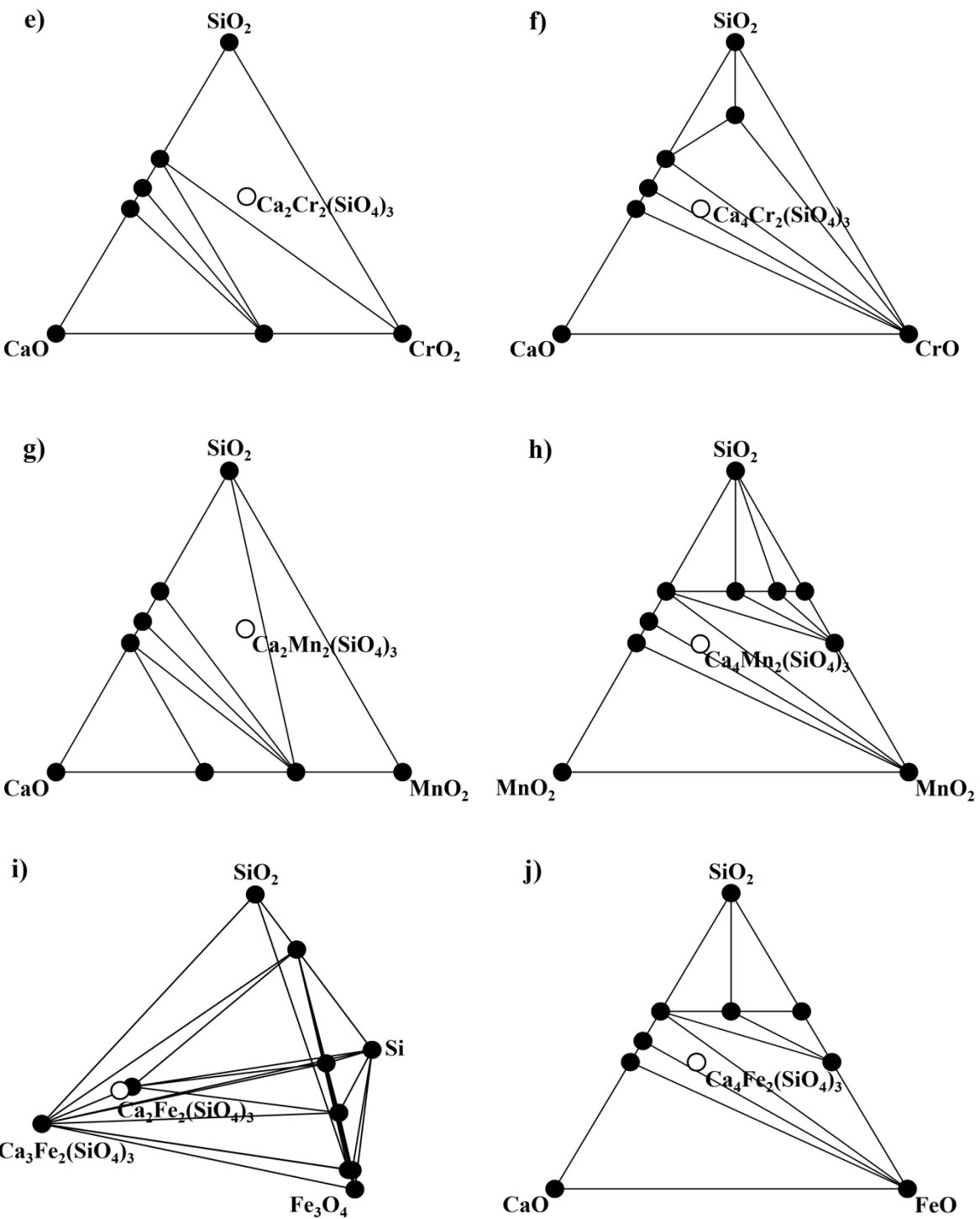


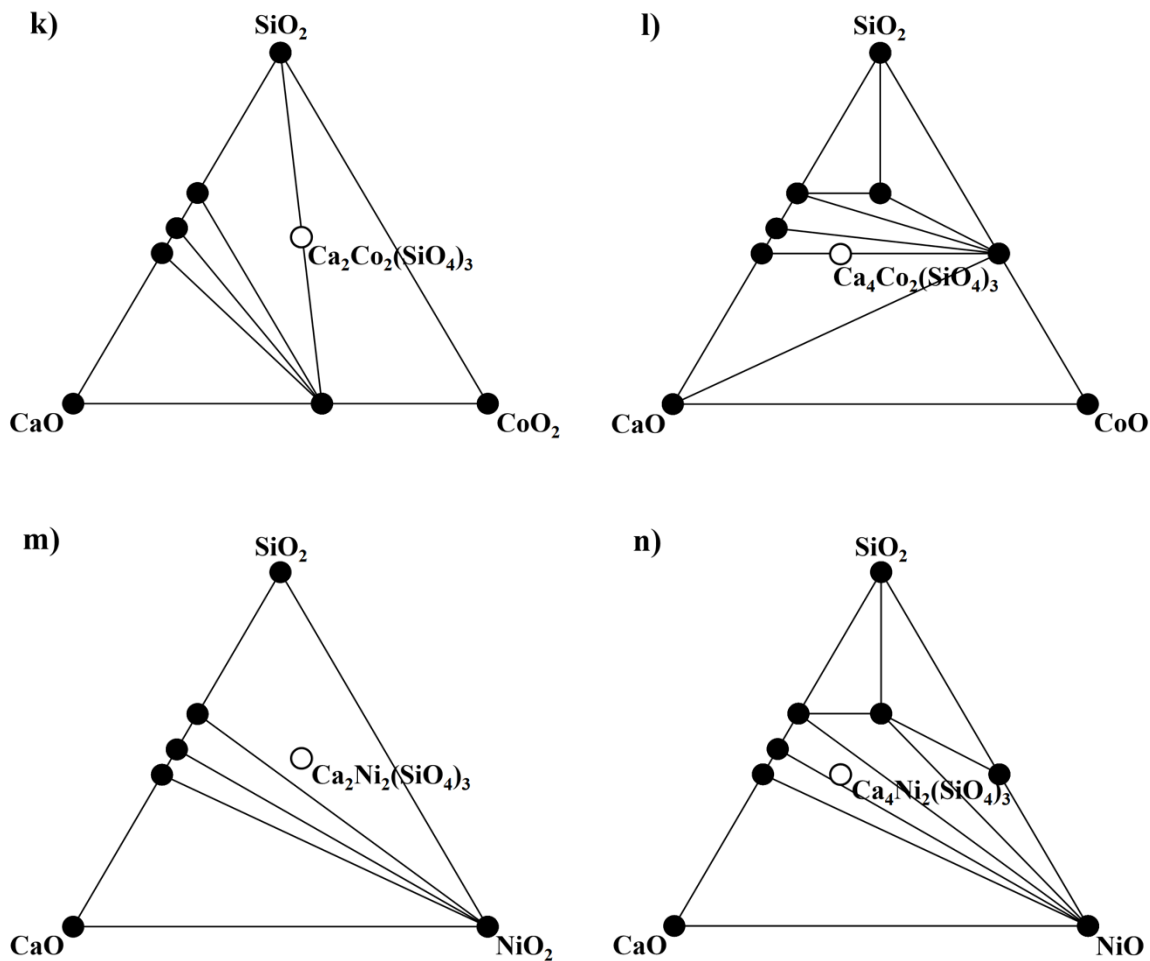
**Figure S4:** Simulated XRD patterns of charged (panels a, c, e, g, i, k, m) and discharged (b, d, f, h, j, l, n) Ti, V, Cr, Mn, Fe, Co, and Ni sulfate Ca-NaSICONs. Notations in the figure are identical to **Figure S2**.

## 0 K phase diagrams of silicate, phosphate, and sulfate Ca-NaSICONs

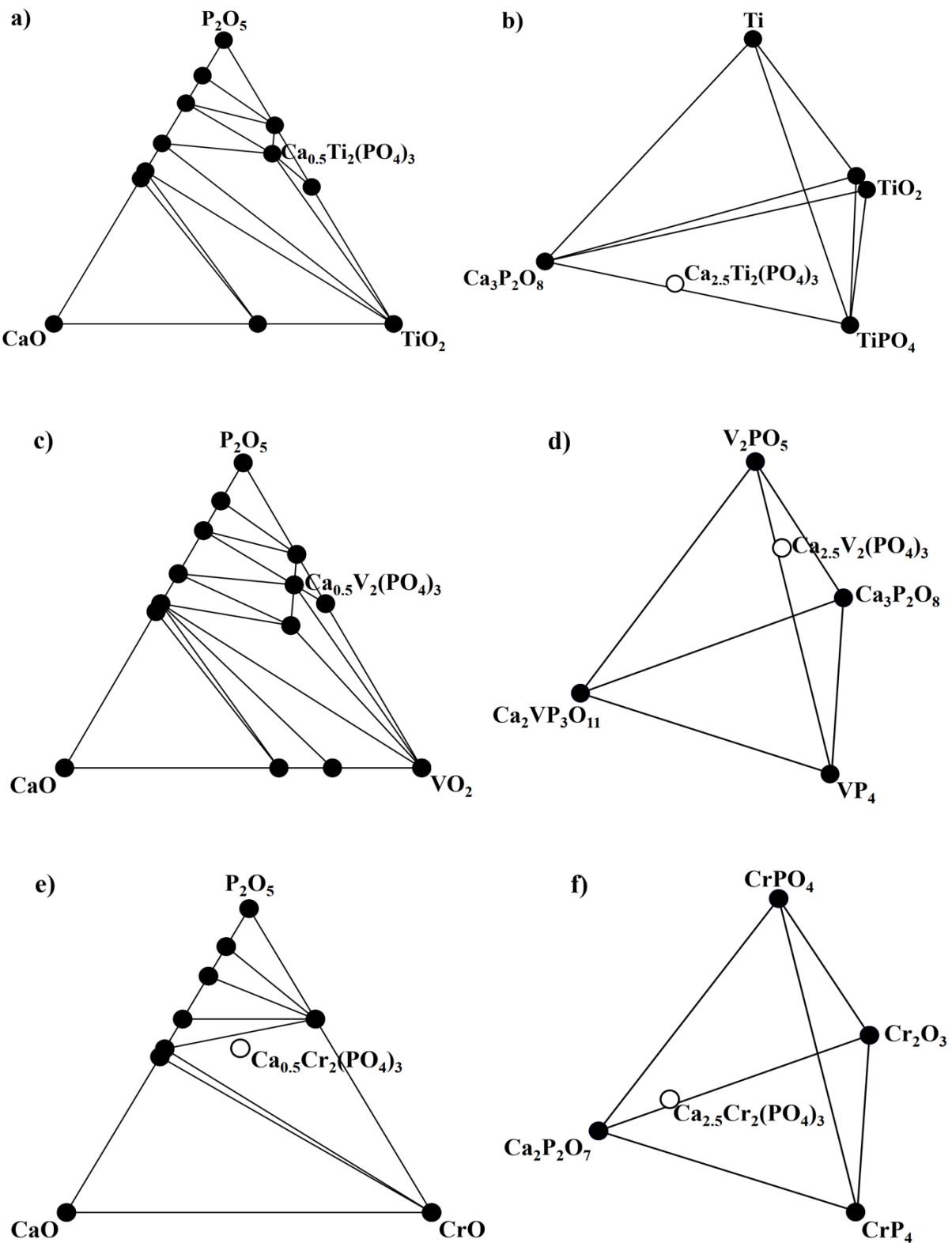
We present the computed 0 K phase diagram of charged and discharged 3d TMs based silicates, phosphates, and sulfates Ca-NaSICONs that were used to investigate their thermodynamic stability in **Figure S5-S7**. We considered the elements, and binary, ternary, and quaternary compounds for the phase diagram construction. For simplicity of visualisation, we display pseudo-ternary and pseudo-quaternary phase diagrams for Ca-NaSICONs for most systems.

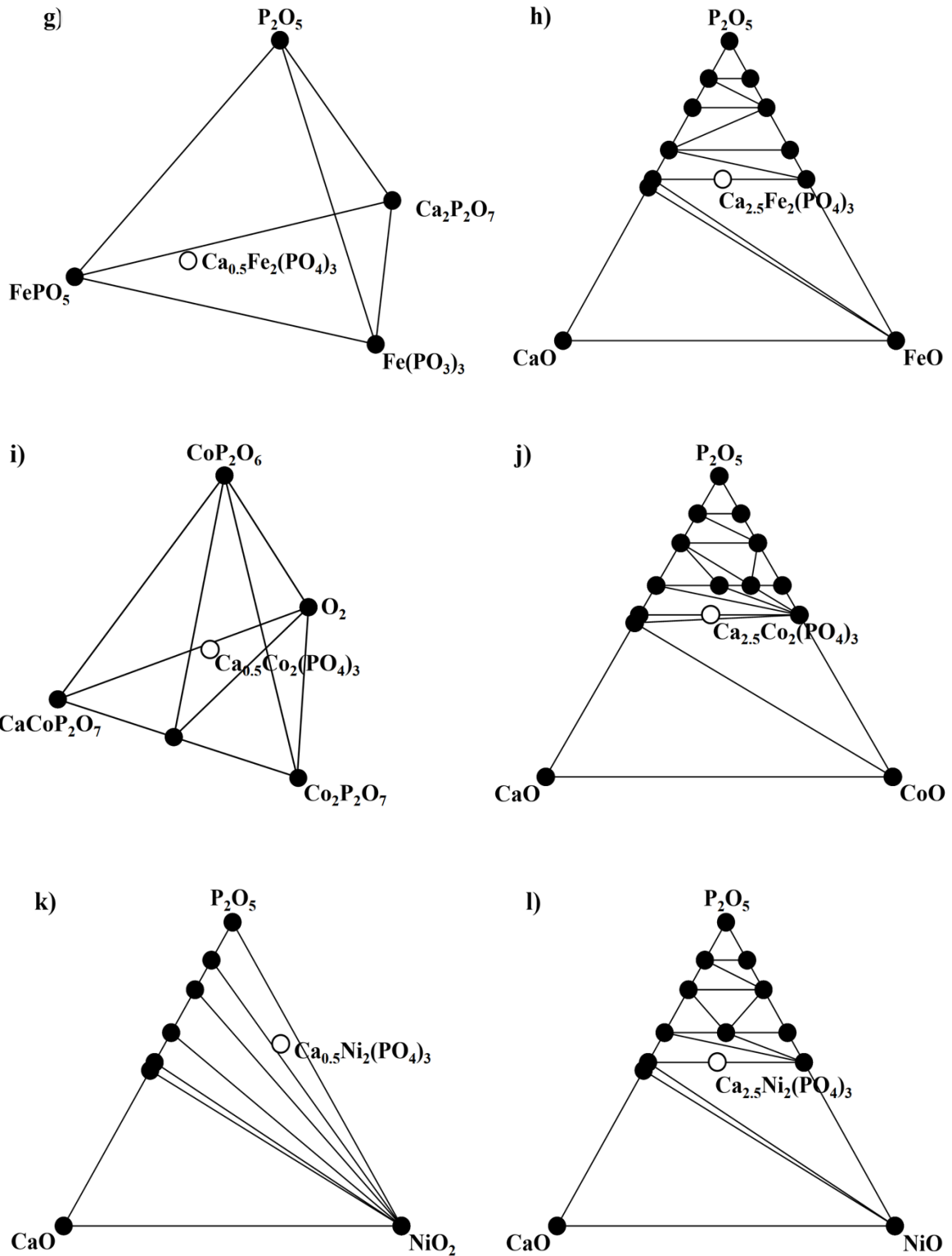




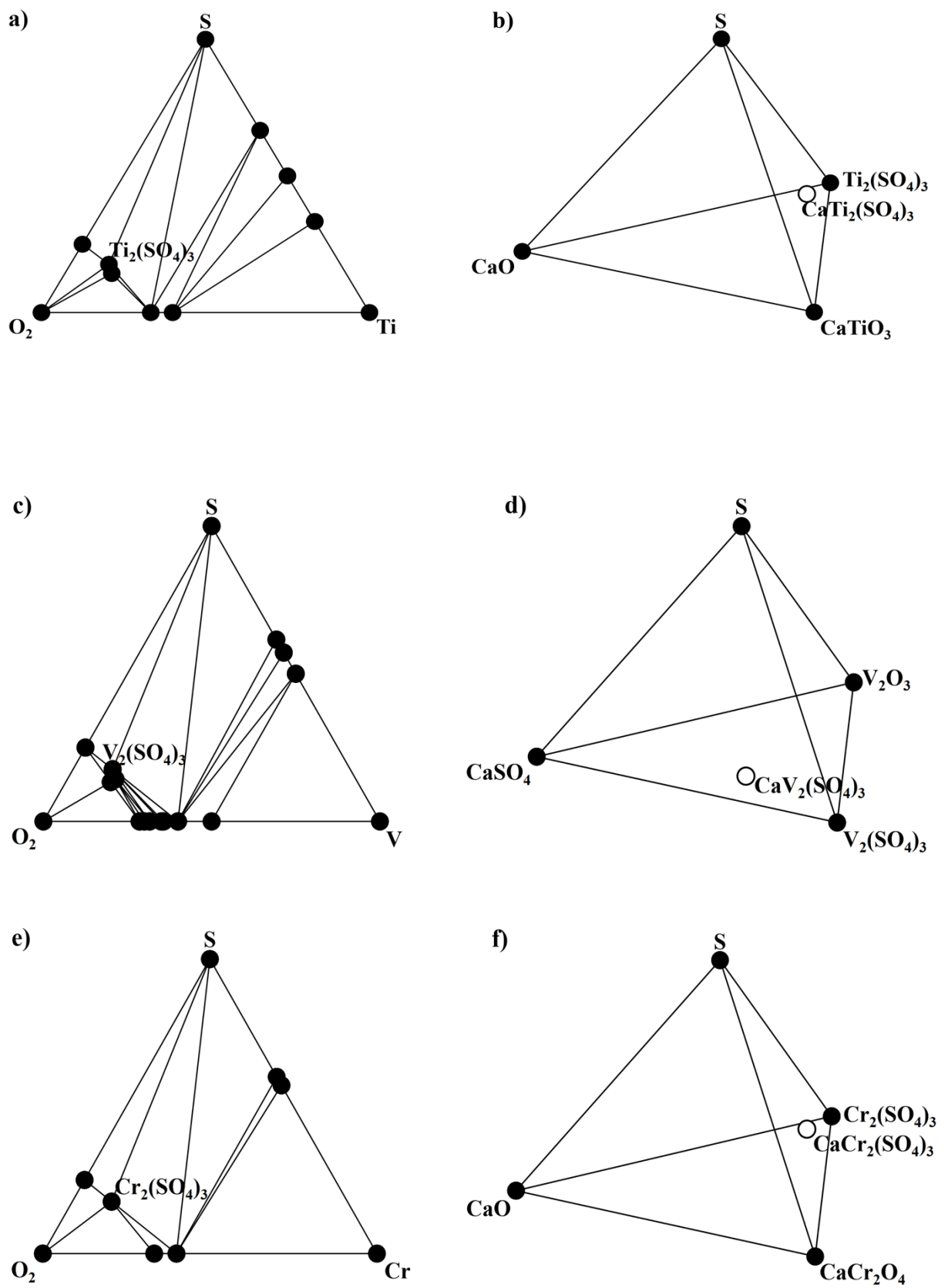


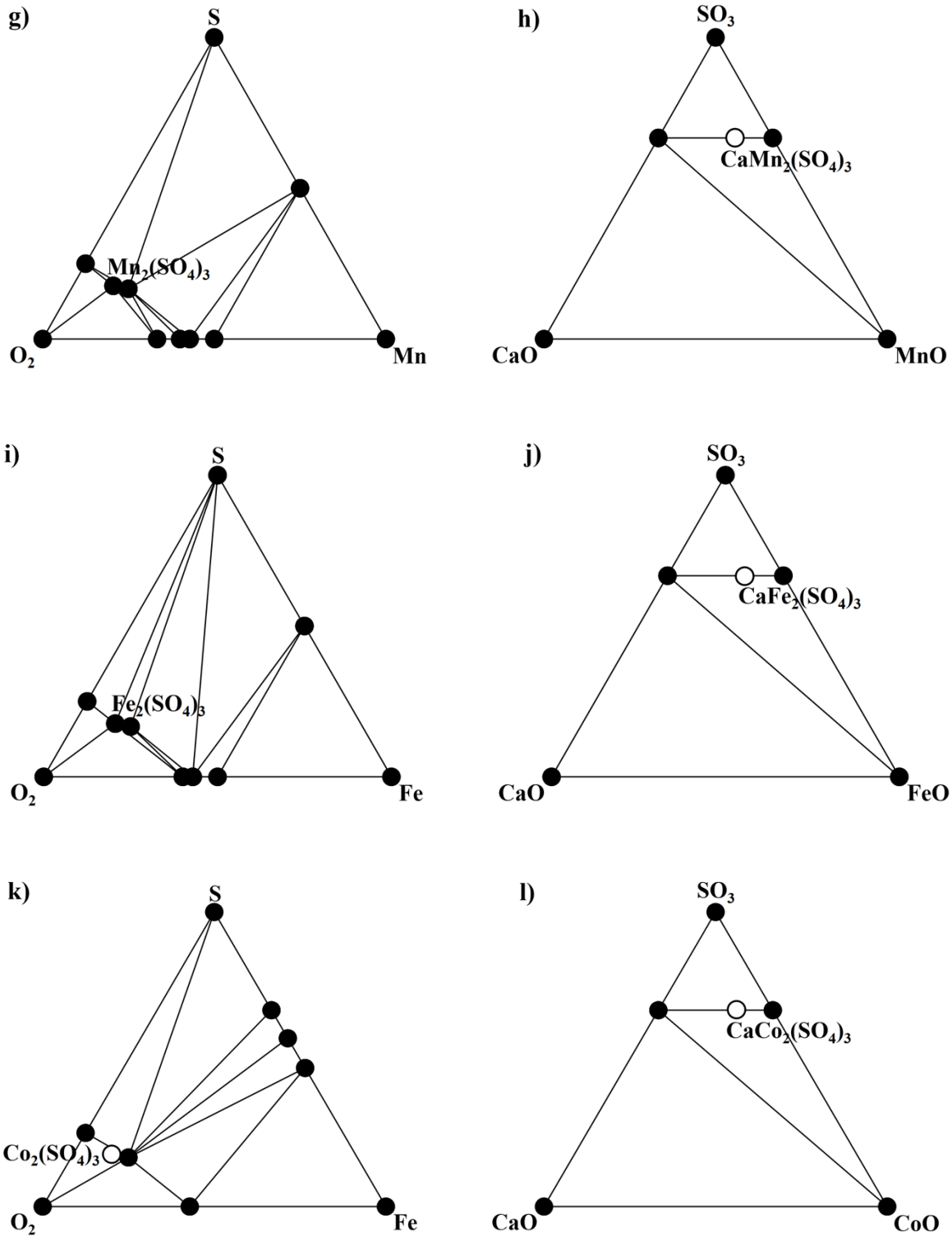
**Figure S5** Phase diagrams of charged (panels a, c, e, g, i, k, m) and discharged (b, d, f, h, j, l, n) Ti, V, Cr, Mn, Fe, Co, and Ni silicate Ca-NaSICONs. Stable entities within each phase diagram are indicated by solid black circles, while solid black lines indicate tie-lines. Unstable/metastable Ca-NaSICONs (i.e., lying above the convex hull) are indicated by hollow black circles.





**Figure S6** Phase diagrams of charged (panels a, c, e, g, i, k) and discharged (b, d, f, h, j, l) Ti, V, Cr, Fe, Co, and Ni phosphate Ca-NaSICONs, respectively. Notations in the figure are identical to **Figure S5**.





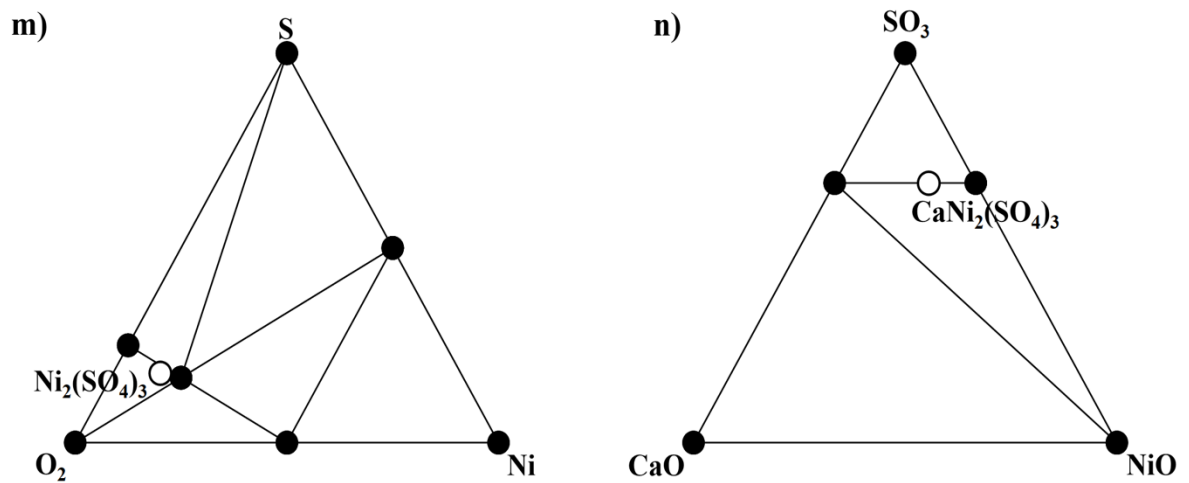


**Figure S7** Phase diagrams of charged (panels a, c, e, g, i, k, m) and discharged (b, d, f, h, j, l, n) Ti, V, Cr, Mn, Fe, Co, and Ni sulfates Ca-NaSICONs. Notations in the figure are identical to **Figure S5**.

**Table S1:** The predicted decomposition products for all unstable or metastable Ca-NaSICONs are presented.

No.	Ca-NaSICON	Decomposition products
<b>Silicates</b>		
1	$\text{Ca}_2\text{Ti}_2(\text{SiO}_4)_3$	$\text{CaTiSiO}_5$ , $\text{SiO}_2$
	$\text{Ca}_4\text{Ti}_2(\text{SiO}_4)_3$	$\text{CaSiO}_3$ , $\text{Ti}_2\text{O}_3$ , $\text{Ca}_3\text{Si}_2\text{O}_7$ , $\text{Ca}_3\text{SiO}$
2	$\text{Ca}_2\text{V}_2(\text{SiO}_4)_3$	$\text{Ca}_3\text{V}_2\text{Si}_3\text{O}_{12}$ , $\text{V}_5\text{O}_9$ , $\text{Ca}_2\text{V}_2\text{O}_7$ , $\text{SiO}_2$
	$\text{Ca}_4\text{V}_2(\text{SiO}_4)_3$	$\text{CaSiO}_3$ , $\text{Ca}_3\text{Si}_2\text{O}_7$ , $\text{VO}$
3	$\text{Ca}_2\text{Cr}_2(\text{SiO}_4)_3$	$\text{Ca}_3\text{Cr}_2\text{Si}_2\text{O}_{12}$ , $\text{Cr}_2\text{O}_3$ , $\text{Cr}$ , $\text{SiO}_2$
	$\text{Ca}_4\text{Cr}_2(\text{SiO}_4)_3$	$\text{Ca}_3\text{Cr}_2\text{Si}_2\text{O}_{12}$ , $\text{Ca}_3\text{SiO}$ , $\text{Cr}$ , $\text{SiO}_2$
4	$\text{Ca}_2\text{Mn}_2(\text{SiO}_4)_3$	$\text{CaSiO}_3$ , $\text{Ca}_2\text{Mn}_3\text{O}_8$ , $\text{SiO}_2$
	$\text{Ca}_4\text{Mn}_2(\text{SiO}_4)_3$	$\text{Mn}_5\text{Si}_3\text{O}_{12}$ , $\text{Ca}_2\text{SiO}_4$ , $\text{Mn}$
5	$\text{Ca}_2\text{Fe}_2(\text{SiO}_4)_3$	$\text{Ca}_3\text{Fe}_2\text{Si}_3\text{O}_{12}$ , $\text{Fe}_2\text{O}_3$ , $\text{O}_2$ , $\text{SiO}_2$
	$\text{Ca}_4\text{Fe}_2(\text{SiO}_4)_3$	$\text{CaSiO}_3$ , $\text{FeO}$ , $\text{Ca}_3\text{Si}_2\text{O}_7$
6	$\text{Ca}_2\text{Co}_2(\text{SiO}_4)_3$	$\text{CaSiO}_3$ , $\text{CaCo}_2\text{O}_4$ , $\text{O}_2$ , $\text{SiO}_2$
	$\text{Ca}_4\text{Co}_2(\text{SiO}_4)_3$	$\text{Ca}_2\text{SiO}_4$ , $\text{Co}_2\text{SiO}_4$
7	$\text{Ca}_2\text{Ni}_2(\text{SiO}_4)_3$	$\text{CaSiO}_3$ , $\text{CaNiSi}_2\text{O}_6$ , $\text{O}_2$ , $\text{NiO}$
	$\text{Ca}_4\text{Ni}_2(\text{SiO}_4)_3$	$\text{Ca}_3\text{Si}_2\text{O}_7$ , $\text{CaSiO}_3$ , $\text{NiO}$
<b>Phosphates</b>		
8	$\text{Ca}_{2.5}\text{Ti}_2(\text{PO}_4)_3$	$\text{TiPO}_4$ , $\text{Ca}_3\text{P}_2\text{O}_8$ , $\text{TiO}_2$ , $\text{Ti}_2\text{P}$
9	$\text{Ca}_{2.5}\text{V}_2(\text{PO}_4)_3$	$\text{Ca}_2\text{VP}_3\text{O}_{11}$ , $\text{VP}_4$ , $\text{V}_2\text{PO}_5$ , $\text{Ca}_3\text{P}_2\text{O}_8$
10	$\text{Ca}_{0.5}\text{Cr}_2(\text{PO}_4)_3$	$\text{Cr}_2\text{P}_4\text{O}_{13}$ , $\text{CaCrO}_4$ , $\text{O}_2$
	$\text{Ca}_{2.5}\text{Cr}_2(\text{PO}_4)_3$	$\text{CrP}_4$ , $\text{CrPO}_4$ , $\text{Ca}_2\text{P}_2\text{O}_7$ , $\text{Cr}_2\text{O}_3$
11	$\text{Ca}_{0.5}\text{Fe}_2(\text{PO}_4)_3$	$\text{FePO}_4$ , $\text{FeP}_3\text{O}_9$ , $\text{Ca}_2\text{P}_2\text{O}_7$ , $\text{O}_2$
	$\text{Ca}_{2.5}\text{Fe}_2(\text{PO}_4)_3$	$\text{Fe}_3\text{P}_2\text{O}_8$ , $\text{Ca}_3\text{P}_2\text{O}_8$
12	$\text{Ca}_{0.5}\text{Co}_2(\text{PO}_4)_3$	$\text{CaCo}_3\text{P}_4\text{O}_{14}$ , $\text{CoP}_2\text{O}_6$ , $\text{O}_2$
	$\text{Ca}_{2.5}\text{Co}_2(\text{PO}_4)_3$	$\text{Ca}_3\text{P}_2\text{O}_8$ , $\text{Co}_3\text{P}_2\text{O}_8$

13	$\text{Ca}_{0.5}\text{Ni}_2(\text{PO}_4)_3$	$\text{P}_2\text{O}_5$ , $\text{NiP}_4\text{O}_{11}$ , $\text{CaNi}_3\text{P}_2\text{O}_{14}$ , $\text{Ni}_6\text{P}$
	$\text{Ca}_{2.5}\text{Ni}_2(\text{PO}_4)_3$	$\text{CaP}_3$ , $\text{Ca}_{10}\text{P}_6\text{O}_{25}$ , $\text{CaNi}_3\text{P}_2\text{O}_{14}$ , $\text{CaP}$
<b>Sulfates</b>		
14	$\text{CaTi}_2(\text{SO}_4)_3$	$\text{CaSO}_4$ , $\text{Ti}_2\text{S}_3\text{O}_{12}$ , $\text{TiO}_2$ , $\text{S}$
15	$\text{CaV}_2(\text{SO}_4)_3$	$\text{V}_2\text{O}_3$ , $\text{V}_2\text{S}_3\text{O}_{12}$ , $\text{CaSO}_4$ , $\text{S}$
16	$\text{CaCr}_2(\text{SO}_4)_3$	$\text{Cr}_2\text{S}_3\text{O}_{12}$ , $\text{CaSO}_4$ , $\text{Cr}_2\text{O}_3$ , $\text{S}$
17	$\text{CaMn}_2(\text{SO}_4)_3$	$\text{MnSO}_4$ , $\text{CaSO}_4$
18	$\text{CaFe}_2(\text{SO}_4)_3$	$\text{FeSO}_4$ , $\text{CaSO}_4$
19	$\text{Co}_2(\text{SO}_4)_3$	$\text{CoSO}_4$ , $\text{O}_2$ , $\text{SO}_3$
	$\text{CaCo}_2(\text{SO}_4)_3$	$\text{CoSO}_4$ , $\text{CaSO}_4$
20	$\text{Ni}_2(\text{SO}_4)_3$	$\text{NiSO}_4$ , $\text{O}_2$ , $\text{SO}_3$
	$\text{CaNi}_2(\text{SO}_4)_3$	$\text{NiSO}_4$ , $\text{CaSO}_4$

**Table S2:** The predicted adjacent phases for all stable Ca-NaSICONs are presented. Note that for all stable entities on a phase diagram, energy below the convex hull represents the formation energy of the stable phase with respect to the adjacent stable phases on the convex hull.

No.	Ca-NaSICON	Adjacent phases
<b>Phosphates</b>		
1	$\text{Ca}_{0.5}\text{Ti}_2(\text{PO}_4)_3$	$\text{Ca}_2\text{P}_2\text{O}_7$ , $\text{Ti}_5\text{P}_4\text{O}_{20}$ , $\text{TiP}_2\text{O}_7$
2	$\text{Ca}_{0.5}\text{V}_2(\text{PO}_4)_3$	$\text{CaV}_2\text{P}_2\text{O}_{10}$ , $\text{VP}_2\text{O}_7$
3	$\text{Ca}_{0.5}\text{Mn}_2(\text{PO}_4)_3$	$\text{MnO}_2$ , $\text{MnP}_3\text{O}_9$ , $\text{Ca}_2\text{P}_2\text{O}_7$ , $\text{O}_2$
	$\text{Ca}_{2.5}\text{Mn}_2(\text{PO}_4)_3$	$\text{MnP}_3\text{O}_9$ , $\text{Ca}_2\text{P}_2\text{O}_7$ , $\text{Mn}_3\text{O}_4$ , $\text{Mn}_2\text{P}$
<b>Sulphates</b>		
4	$\text{Ti}_2(\text{SO}_4)_3$	$\text{TiO}_5\text{S}$ , $\text{SO}_3$ , $\text{S}$
5	$\text{V}_2(\text{SO}_4)_3$	$\text{SO}_3$ , $\text{VO}_5\text{S}$ , $\text{S}$
6	$\text{Cr}_2(\text{SO}_4)_3$	$\text{SO}_3$ , $\text{Cr}_2\text{O}_3$
7	$\text{Mn}_2(\text{SO}_4)_3$	$\text{SO}_3$ , $\text{MnSO}_4$ , $\text{O}_2$
8	$\text{Fe}_2(\text{SO}_4)_3$	$\text{SO}_3$ , $\text{FeSO}_4$ , $\text{O}_2$

## Migration barriers of Ca-NaSICONs: minimum energy pathways (MEPs)

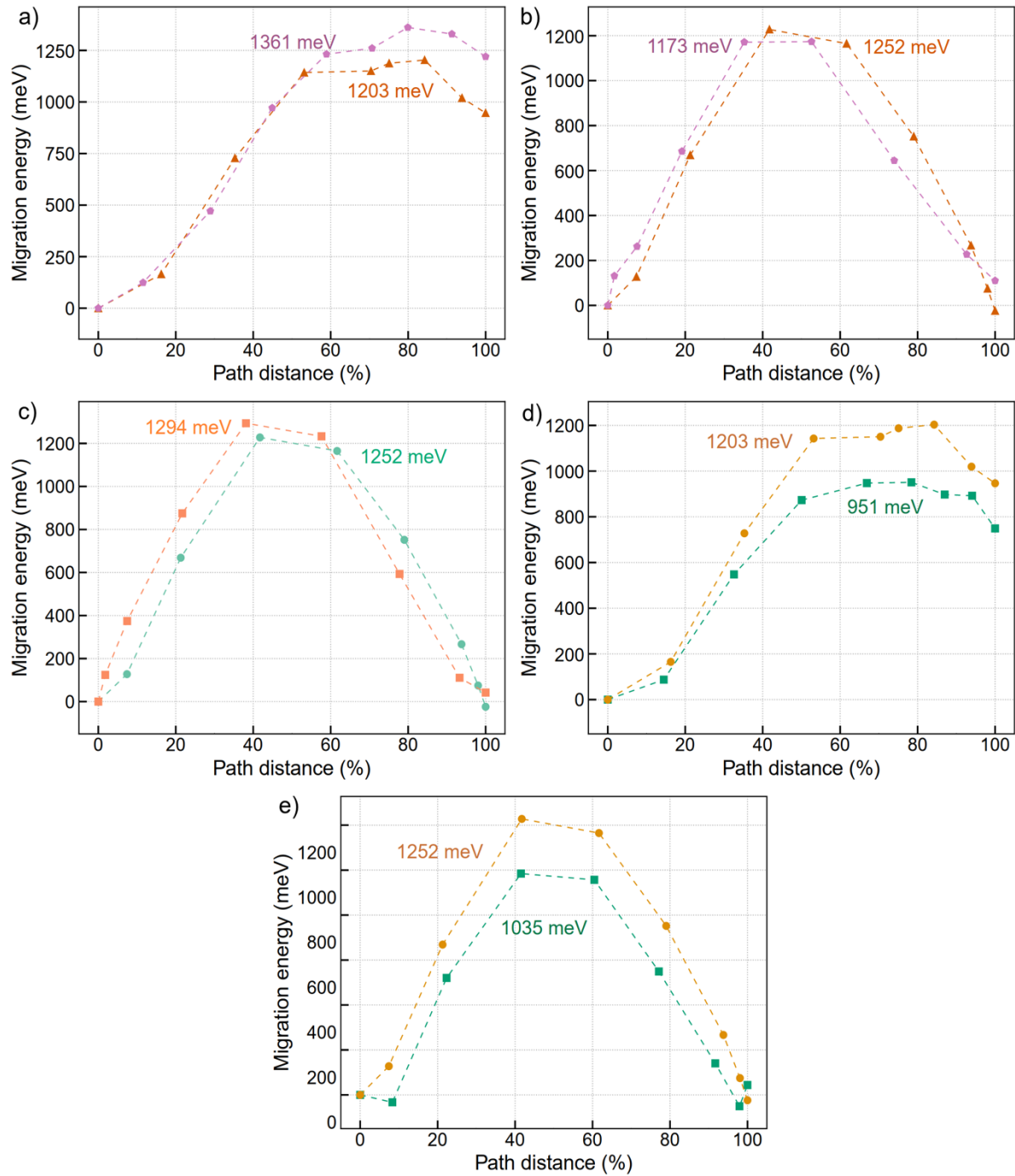


**Figure S8:** The strongly constrained and appropriately normed (SCAN)-calculated Ca<sup>2+</sup> minimum energy pathways (MEPs) and migration barrier ( $E_m$ ) comparison in a primitive Ca-NaSICON cell (dark orange triangle, 2 M<sub>2</sub>(ZO<sub>4</sub>)<sub>3</sub> formula units) versus supercell (violet pentagon, 8 formula units) of charged (panel a) and discharged (panel b) V-phosphate, respectively. (c) SCAN (light green circle) versus SCAN with Hubbard correction (SCAN+U) (light orange square)-calculated  $E_m$  for primitive cell of Ca<sub>2.5</sub>V<sub>2</sub>(PO<sub>4</sub>)<sub>3</sub>. (d, e) Generalized gradient approximation (GGA) (green squares) versus SCAN (dark orange circles)-calculated  $E_m$  for charged (d) and discharged (e) Ca<sub>x</sub>V<sub>2</sub>(PO<sub>4</sub>)<sub>3</sub> NaSICONs done within the primitive cell. The  $E_m$  values are listed as a text annotation with the same colour as their respective symbols.

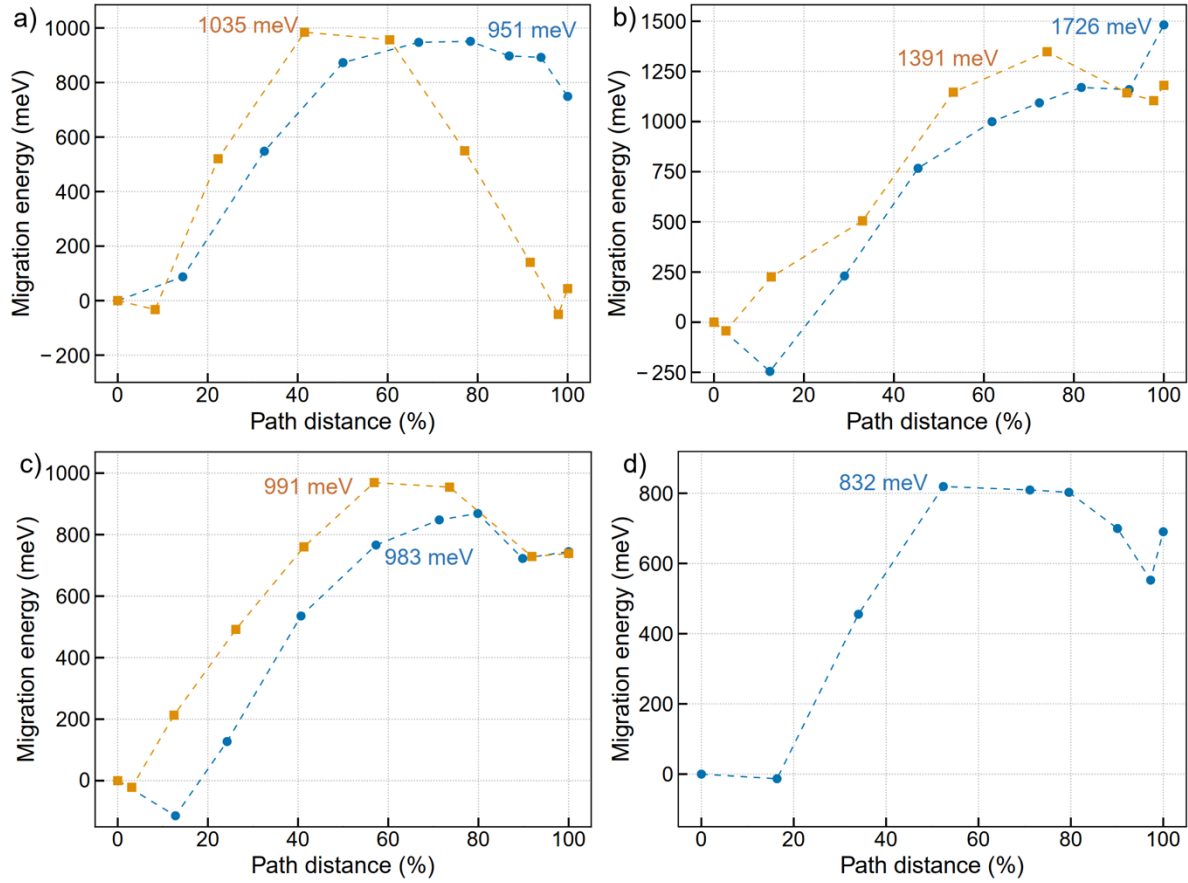


**Figure S9:** The MEPs of  $\text{Ca}^{2+}$  migration calculated using GGA for the candidate Ca-NaSICONs, namely, (a)  $\text{Ca}_x\text{V}_2(\text{PO}_4)_3$ , (b)  $\text{Ca}_x\text{Mn}_2(\text{PO}_4)_3$ , (c)  $\text{Ca}_x\text{Mn}_2(\text{SO}_4)_3$ , and (d)  $\text{Ca}_x\text{Fe}_2(\text{SO}_4)_3$ . The charged and discharged compositions in each panel are represented by the blue circles and orange squares, respectively and the  $E_m$  values are listed as a text annotation with the same colour as their respective symbols. Note that the data for discharged Fe-sulphate is not presented here due to convergence difficulties of the nudged elastic band (NEB) calculation.

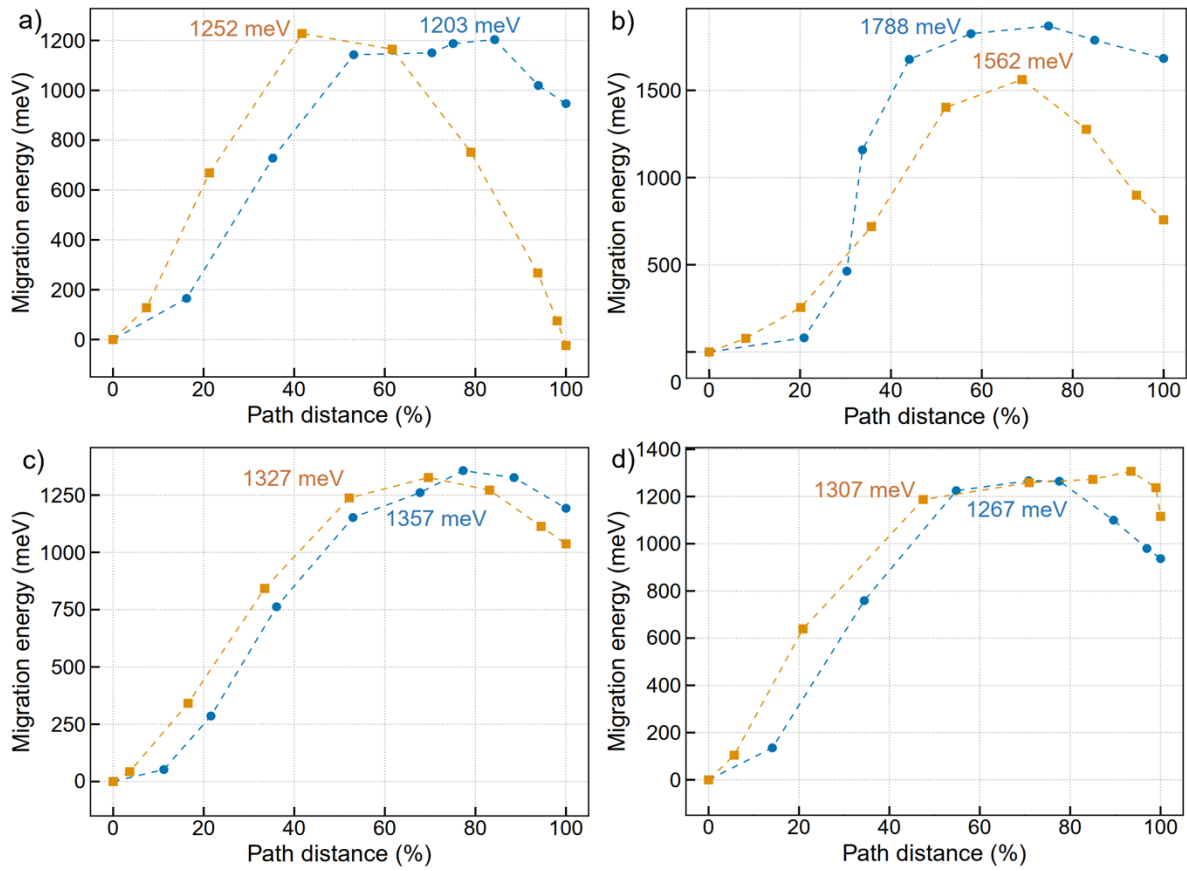


**Figure S10:** The MEPs of  $\text{Ca}^{2+}$  migration calculated using SCAN functional for the candidate Ca-NaSICONs, namely, (a)  $\text{Ca}_x\text{V}_2(\text{PO}_4)_3$ , (b)  $\text{Ca}_x\text{Mn}_2(\text{PO}_4)_3$ , (c)  $\text{Ca}_x\text{Mn}_2(\text{SO}_4)_3$ , and (d)  $\text{Ca}_x\text{Fe}_2(\text{SO}_4)_3$ . Notations in the figure are identical to **Figure S9**.

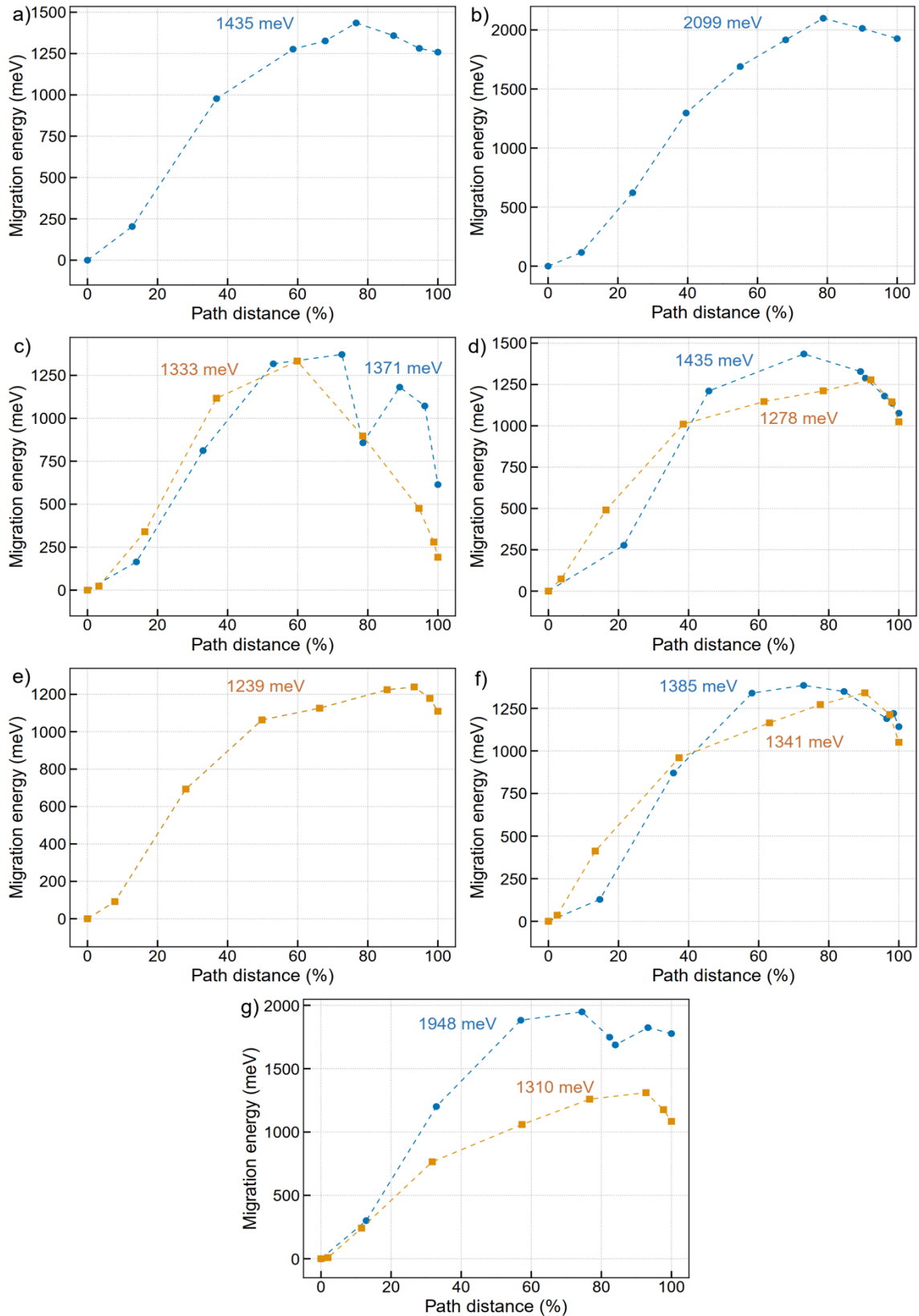


**Figure S11:** The MEPs of Ca-migration calculated using SCAN for (a)  $\text{Ca}_{0.5}\text{Cr}_2(\text{PO}_4)_3$ , (b)  $\text{Ca}_{0.5}\text{Fe}_2(\text{PO}_4)_3$ , (c)  $\text{Ca}_x\text{Co}_2(\text{PO}_4)_3$ , (d)  $\text{Ca}_x\text{V}_2(\text{SO}_4)_3$ , (e)  $\text{CaCr}_2(\text{SO}_4)_3$ , (f)  $\text{Ca}_x\text{Co}_2(\text{SO}_4)_3$ , and (g)  $\text{Ca}_{2.5}\text{Ni}_2(\text{SO}_4)_3$ . In panels c, d, f, and g, the charged (discharged) Ca-NaSiCON compositions are indicated by blue circles (orange squares). Notations in the figure are identical to **Figure S9**. The MEP data for  $\text{Ca}_{2.5}\text{Cr}_2(\text{PO}_4)_3$ ,  $\text{Ca}_{2.5}\text{Fe}_2(\text{PO}_4)_3$ , and  $\text{Cr}_2(\text{SO}_4)_3$  are not presented due to convergence difficulties.

**Table S3:** The comparison of calculated  $E_m$  with respect to the choice of the exchange-correlation functional (i.e., GGA, SCAN and SCAN+U) and cell size (i.e., primitive cell and supercell with 8 formula units of  $M_2(ZO_4)_3$ ) by using  $Ca_xV_2(PO_4)_3$  as a test. The difference in  $E_m$  between SCAN and SCAN+U appears insignificant, while GGA gives the lowest  $E_m$  value. The  $E_m$  change between primitive and supercell also appears to be minimal.

Primitive cell vs. Supercell			
Compositions	Migration Barriers (meV)	Functional type	Cell type
$Ca_{0.5}V_2(PO_4)_3$	1,203	SCAN	Primitive
$Ca_{0.5}V_2(PO_4)_3$	1,361	SCAN	Supercell
$Ca_{2.5}V_2(PO_4)_3$	1,252	SCAN	Primitive
$Ca_{2.5}V_2(PO_4)_3$	1,173	SCAN	Supercell
SCAN vs. SCAN+U			
$Ca_{2.5}V_2(PO_4)_3$	1,252	SCAN	Primitive
$Ca_{2.5}V_2(PO_4)_3$	1,294	SCAN+U	Primitive
GGA vs. SCAN			
$Ca_{0.5}V_2(PO_4)_3$	951	GGA	Primitive
$Ca_{0.5}V_2(PO_4)_3$	1,203	SCAN	Primitive
$Ca_{2.5}V_2(PO_4)_3$	1,035	GGA	Primitive
$Ca_{2.5}V_2(PO_4)_3$	1,252	SCAN	Primitive